Diffusion and Sedimentation Studies on Poly(macromonomer) in Dilute Solution

Norio Nemoto,*,† Masahiro Nagai,‡ Akihiro Koike,‡ and Sinichi Okada‡

Department of Applied Physics, Faculty of Engineering, Kyushu University, Hakozaki, Fukuoka 812, Japan, and Institute for Chemical Research, Kyoto University, Uji, Kyoto 611, Japan

Received December 28, 1994; Revised Manuscript Received March 13, 1995®

ABSTRACT: Dynamic light scattering and sedimentation velocity measurements were performed on dilute benzene solutions of poly(macromonomer) with poly(methyl methacrylate) (PMMA) as the backbone chain and polystyrene (PS) as branches to obtain the diffusion coefficient D and the sedimentation coefficient s, respectively. Dependences of D and s at infinite dilution on the backbone chain length as well as the branch length were found to be quantitatively described by the prolate ellipsoid model with values of the main and the minor axis calculated from the planar zigzag PMMA backbone and the gaussian PS branched chains, respectively. Application of the wormlike cylinder model gave the Kuhn's statistical length λ^{-1} $\sim$ 90 nm, which is substantially larger than $\lambda^{-1} = 3.2$ nm of homo-PMMA. The concentration coefficient of D and s also showed unique dependences on the backbone chain length as well as the branch length.

Introduction

Effects of branching on polymer chain dynamics in dilute solution have been studied so far using branched polymer with three different types of branched structures such as randomly-branched, star-shaped, and comb-shaped polymers.[1–6] In the latter two systems, attention was focused on the effect of high monomer density in the vicinity of the branching point(s) on hydrodynamic properties such as steady viscosity and diffusion coefficient. On the other hand, novel new types of multibranched polymers such as poly(macromonomer) and dendrimer have recently become available due to advancement of polymerization techniques, and their characterization has just started.[7–16]

The poly(macromonomer) with the number of branches the same as its degree of polymerization has the following characteristic features: (1) the branch length can be made fairly uniform using the anionic polymerization technique, (2) branching regularly occurs along the chain backbone, for example, every two carbon atoms for vinyl types of polymers, and, consequently, (3) monomer density is very high around the chain backbone. The effect of this unique multibranched structure on hydrodynamic properties has been discussed in terms of intrinsic viscosity by Tsukahara and his co-workers.[17]

In order to get more information on chain dynamics of the poly(macromonomer), we performed dynamic light scattering and sedimentation velocity measurements on dilute benzene solutions of two series of poly(macromonomer) with poly(methyl methacrylate) (PMMA) as the backbone and polystyrene (PS) as branches. Analysis of diffusion and sedimentation data with a couple of models indicates that the PMMA backbone is quite stiff as is given by Kuhn's statistical length $\lambda^{-1} \sim$ 90 nm, while the PS branches take a conformation close to that of a Gaussian chain. When we had almost finished the measurements, we became aware of the fact that Schmidt and his group made static and dynamic light scattering experiments on the same system.[18] It is gratifying that their conclusions are in good agreement with ours.

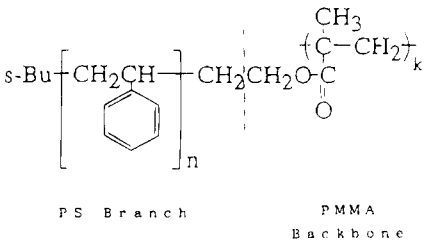

Figure 1. Chemical formula of the poly(macromonomer) used.

Experimental Section

Materials. The poly(macromonomer) used in this study is a gift of Prof. Tsukahara of Kyoto Institute of Technology. As the chemical formula in Figure 1 shows, the macromonomer is [ω-(methacryloyloxy)ethyl]polystyrene synthesized by living anionic polymerization. The macromonomers were polymerized using AIBN as an initiator in benzene at 60 °C for 24 h, and the products were then purified by precipitation–extraction procedures to remove unreacted macromonomers.[8] In order to study the effects of the backbone chain length and the branch length on polymer dynamics, two series of samples were prepared. For one series of samples, the molecular weight of the PS branch was fixed at 2900 with a ratio of the weight- to number-average molecular weight of 1.06, and the degree of polymerization, DP_{PMMA}, of the PMMA backbone was varied from 5.7 to 1019 for six samples tested. For a second series of samples, DP_{PMMA} was kept at around 20 and the weight-average molecular weight of the PS branch was varied from 800 to 14 000. Table 1 gives the sample code, weight-average molecular weight of the macromonomer, the total weight-average molecular weight, M_w, and M_n of the poly(macromonomer) samples used.

Dilute solutions of the poly(macromonomer) in benzene were prepared by mixing a prescribed amount of the pure solvent and of a polymer solution of known concentration and made optically clean by filtration with Millipore filters (nominal pore size, 0.22 μm).

Methods. Dynamic light scattering (DLS) measurements were performed using the apparatus described in detail elsewhere.[19] A vertically polarized single-frequency 488 nm line of an argon ion laser (Spectra Physics, Beamlock 2060) was used as a light source with an output power of 600 mW. The normalized time correlation function $A_q(t)$ of the vertical component of the light intensity scattered from solutions was measured using the digital correlators (Otsuka Electronics and

* To whom correspondence should be addressed.
† Kyushi University.
‡ Kyoto University.
® Abstract published in *Advance ACS Abstracts,* April 15, 1995.

0024-9297/95/2228-3854$09.00/0

Table 1. Characteristics of Poly(macromonomer) Samples

sample code (X and Y)	M_w of macromonomer	DP_{PMMA}	M_w of poly(macromonomer)/10^4	M_w/M_n
	PM2900-X Series			
−6	3100	5.7	1.76	1.35
−20	3100	20.2	6.27	1.86
−81	3100	81.0	25.1	1.30
−171	3100	171	52.9	2.52
−212	3100	212	65.7	1.68
−1019	3100	1019	316	1.18
	PM Y-20 Series[a]			
800−22	890	21.9	1.95	1.27
5500−23	6100	22.8	13.9	
14000−19	14600	19.2	28.0	1.75

[a] The second sample of the PM2900-X series was also used for a study of the branch-length effect.

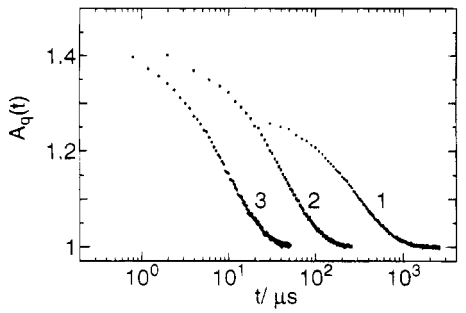

Figure 2. Examples of time profiles of the normalized time correlation function of $A_q(t)$ for the poly(macromonomer) sample PM14000-19 in benzene with $C = 2.0$ mg cm^{-3} at $T = 25.0$ °C. The scattering angles θ are (1) 20°, (2) 55°, and (3) 150°, respectively.

ALV 5000) at 12 scattering angles ranging from 10.4° to 150° at 25 ± 0.05 °C.

Sedimentation velocity (SV) experiments were made at 25 ± 0.05 °C using an analytical ultracentrifuge (Beckman Spinco Model E).

Results

Dynamic Light Scattering (DLS). Time profiles of $A_q(t)$ obtained with an Otsuka correlator showed that distributions of the decay rate Γ were unimodal in the delay time range of 1 μs to 10 ms for all poly(macromonomer) solutions tested at all scattering angles θ. Figure 2 shows an example of $A_q(t)$ for the benzene solution of the PM14000-19 sample at $\theta = 20$, 55, and 150°. The unimodal nature of the Γ distributions was confirmed using the ALV correlator which covers a much wider range of the delay time from 0.1 μs to 10 s. Cumulant analysis was then applied for an estimate of the first cumulant Γ_e as a quantity characteristic of the diffusion behavior of the poly(macromonomer) in dilute solution.

Backbone Chain-Length Dependence of the Translational Diffusion Coefficient D_0. Figure 3 gives a plot of Γ_e/q^2 against q for two polymer samples, where q (=$(4\pi/\lambda)\sin(\theta/2)$; λ, the wavelength of light in the medium) represents the magnitude of the scattering vector **q**. As Figure 3a shows, Γ_e/q^2 of the highest molecular weight sample PM2900-1019 tends to increase with an increase in q. The increase may be attributable to the characteristic geometrical shape of the poly(macromonomer) as will be described later. Though Γ_e/q^2 appears almost independent of q at low q, the data were linearly extrapolated to obtain the mutual diffusion coefficient $D(C)$ defined as $D(C) \equiv (\Gamma_e/q^2)_{q\to 0}$.

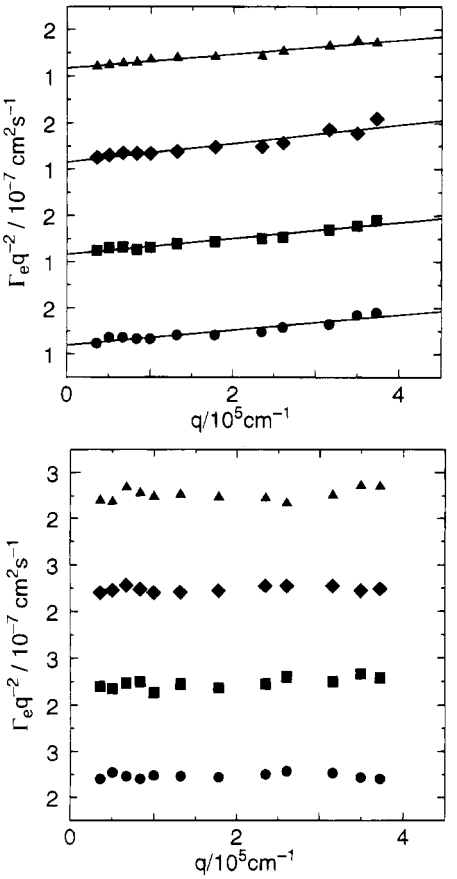

Figure 3. Scattering vector q dependence of the first cumulant Γ_e in the form of $\Gamma_e q^{-2}$ vs q plot for (a) the highest molecular weight sample PM2900-1019 and (b) the sample PM2900-171.

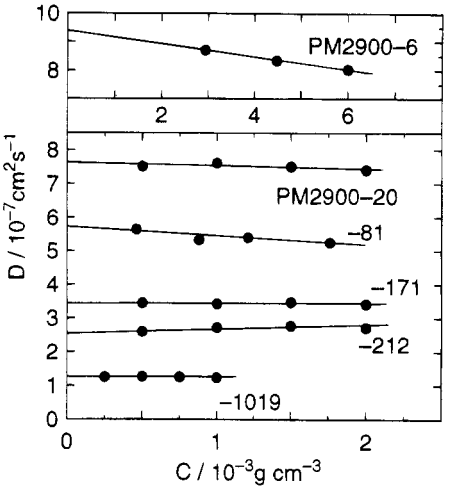

Figure 4. Extrapolation of the mutual diffusion coefficient $D(C)$ to obtain the diffusion coefficient at infinite dilution D_0 and the concentration coefficient k_D for the PM2900 series of samples.

On the other hand, Γ_e/q^2 of other lower molecular weight samples was found to be independent of q as exemplified in Figure 3b. Thus, $D(C)$ was easily estimated as an averaged value of Γ_e/q^2.

The dependence of $D(C)$ on polymer concentration C is shown in Figure 4 for six samples. The concentration dependence of $D(C)$ is weak, and the data are well fitted with the linear eq 1, from which the translational diffusion coefficient D_0 at infinite dilution and concentration coefficient k_D are obtained

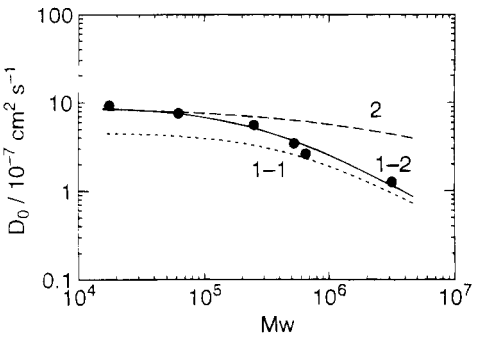

Figure 5. Dependence of D_0 on the PMMA backbone chain length shown as a plot of D_0 against the total weight-average molecular weight M_w of the poly(macromonomer) ($DP_{PMMA} = M_w/3100$) and compared with three curves calculated using three models: (1-1) prolate ellipsoid model 1, (1-2) prolate ellipsoid model 2, and (2) the Gaussian coil model.

Table 2. Experimental Results for D_0, s_0, k_D, and k_s

sample code	$D_0/10^{-7}$ cm^2 s^{-1}	k_D/cm^3 g^{-1}	$s_0/10^{-13}$ s	k_s/cm^3 g^{-1}
PM2900-6	9.39	-24 ± 4	1.73	5 ± 1
PM2900-20	7.61	-12 ± 4	3.98	4 ± 1
PM2900-81	5.45	-21 ± 7	10.4	8 ± 3
PM2900-171	3.45	0 ± 5	13.3	8 ± 2
PM2900-212	2.59	12 ± 5	17.1	12 ± 3
PM2900-1019	1.25	0 ± 5	32.6	70 ± 20
PM800-22	8.45	0 ± 1	2.14	10 ± 2
PM5500-23	5.78	5 ± 2	5.3	50 ± 10
PM14000-19	3.61	17 ± 3	7.7	100 ± 20

and listed in Table 2.

$$D(C) = D_0(1 + k_D C) \quad (1)$$

The k_D changes the sign from a negative to a positive one with increasing M_w. Benzene is a good solvent to both of the PMMA and PS chains which constitute the poly(macromonomer). Therefore, respective homopolymer chains are expanded in benzene due to the excluded-volume effect and give the large second virial coefficient A_2, resulting in large positive k_D values. On the other hand, k_D remains small even at the highest molecular weight sample. The weak C dependence may be related to the unique multibranched structure of the poly(macromonomer) as will be briefly discussed later.

The dependence of D_0 on the backbone chain length is shown as a plot of D_0 against the total weight-average molecular weight M_w of the poly(macromonomer) ($DP_{PMMA} = M_w/3100$) in Figure 5. In the low-M_w region, D_0 only slightly decreases with increasing M_w, while its M_w dependence becomes appreciable in the high-M_w region to an extent similar to that found for linear flexible polymers.[20-23] In taking into account very high monomer density around the backbone, it seems reasonable to consider that the above PMMA backbone length dependence of D_0 may be closely related to chain expansion of either the PMMA backbone or the PS branch, or of both, which determines the shape and the size of the poly(macromonomer) molecule as a whole. We here adopted the prolate ellipsoid model for data analysis, since the model needs only two parameter values of the semimajor and the semiminor axes, a and b, for calculation of D_0 to be compared with experimental values.[24]

$$D_0 = k_B T/f_0 = k_V T/6\pi\eta_0 a G(\varrho) \quad (2)$$

$$G(\varrho) = (1 - \varrho^2)^{1/2}/\ln[(1 + (1 - \varrho^2)^{1/2})/\varrho] \quad (3)$$

where f_0 is the translational friction coefficient of the molecule, η_0 is the solvent viscosity, $\varrho = b/a$ is the axial ratio, and $k_B T$ has its usual meaning. When $a = b = R$, $G(\varrho)$ becomes unity; hence, eq 2 reduces to the Stokes–Einstein equation for a rigid sphere of radius R.

$$D_0 = k_B T/f_0 = k_B T/6\pi\eta_0 R \quad (4)$$

The following three extreme cases were considered as a possible conformation of PMMA and PS chains tentatively.

The prolate ellipsoid model 1-1: the PMMA backbone chain and the PS branches both take a planar zigzag conformation, and a and b are calculated as $2a = L_{PMMA} + 2L_{PS}$ and $b = L_{PS}$ with eq 5.

$$L_i = 0.252 DP_i \text{ nm } (i = \text{PMMA, PS}) \quad (5)$$

The prolate ellipsoid model 1-2: the PMMA backbone chain takes a similar planar zigzag conformation as the model 1-1, while the PS branch is the Gaussian coil. With this model, dimensions of the ellipsoid are calculated as $2a = L_{PMMA} + 2\langle L_{PS}^2\rangle^{1/2}$ and $b = \langle L_{PS}^2\rangle^{1/2}$ using eq 5 for L_{PMMA} and eq 6, a relationship between the root-mean-square end-to-end distance of linear PS in the Θ state, for $\langle L_{PS}^2\rangle^{1/2}$, respectively.[25]

$$\langle L_{PS}^2\rangle^{1/2} = 7.00 \times 10^{-2} M_{PS}^{1/2} \text{ nm} \quad (6)$$

The Gaussian coil model 2: the PMMA backbone chain and the PS branches both take a Gaussian coil form, and the radius of the sphere may be estimated as the sum of the radius of gyration of PMMA R_G with eq 7 and $\langle L_{PS}^2\rangle^{1/2}$ with eq 6.

$$R_G = 2.66 \times 10^{-2} M_{PMMA}^{1/2} \text{ nm} \quad (7)$$

Three curves in the figure are ones calculated with eqs 2–7 for these models. As is clear from the figure, the prolate ellipsoid model 1-2 successfully predicts the backbone chain-length dependence of D_0 over the whole range of M_w in comparison with the other models. It also seems amazing that this simple model could reproduce the absolute magnitude of D_0.

Branch-Length Dependence of D_0. Dynamic light scattering measurements were performed on another series of dilute benzene solutions of poly(macromonomer) samples with $DP_{PMMA} \sim 20$ and M_{PS} ranging from 800 to 14 000. The first cumulant Γ_e obtained from the cumulant analysis of the $A_q(t)$ data was proportional to q^2 over the whole range of q examined, and the mutual diffusion coefficient $D(C)$ was estimated as an average of Γ_e/q^2. The concentration dependence of $D(C)$ was accurately represented by eq 1, from which D_0 and k_D were estimated as listed in Table 2.

Figure 6 gives a logarithmic plot of D_0 (○) against M_w, which are compared with the solid and dashed curves calculated based on the two prolate ellipsoid models with $DP_{PMMA} = 20$, respectively. The branch-length depedence of D_0 as a whole is obviously better represented by the model 1-2 which was successful in describing the backbone chain-length dependence of D_0. However, D_0 of the lowest M_w sample ($M_{PS} = 800$) significantly deviates from the solid curve by about 25%. We recalculated D_0 using DP_{PMMA} values given in Table 1 through eqs 2–6 and show the results (◆) in the same figure. Deviation was not reduced by this procedure. On the other hand, we see that D_0 of the lowest M_w

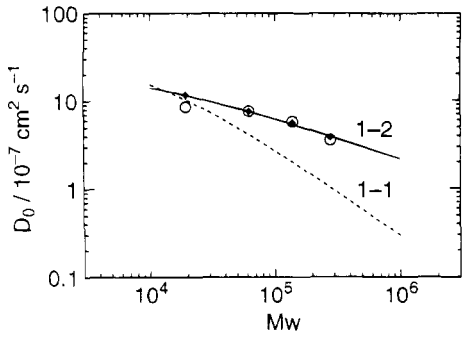

Figure 6. Dependence of D_0 (○) on the PS branch length compared with calculated results using two ellipsoid models, 1-1 and 1-2. Calculated results using true DP_{PMMA} values given in Table 1 are shown by symbols ◆.

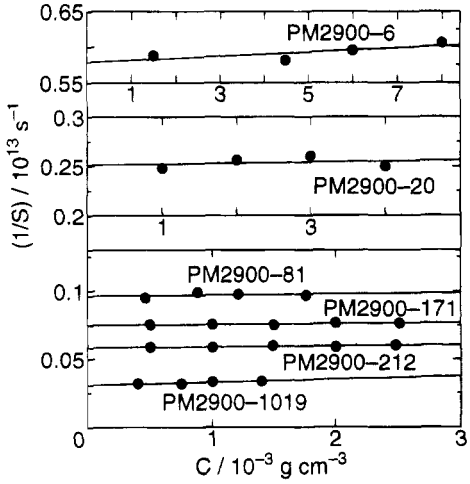

Figure 7. Plot of $s(C)^{-1}$ against C to obtain the sedimentation coefficient at infinite dilution s_0 and the concentration coefficient k_s for the PM2900 series of samples.

sample is pretty close to the dashed curve which was obtained by assuming that the PS branch takes the planar zigzag conformation. This may suggest that several styrene monomer units sprouting from the branching points are forced to be fairly extended, probably vertically to the backbone, owing to very high monomer density in the vicinity of the PMMA backbone characteristic of the poly(macromonomer).

Sedimentation Velocity (SV). Sedimentation velocity experiments were made mostly on the same solutions after being used for DLS measurements. A single peak due to the sedimentation of poly(macromonomer) molecules was observed in photographs of the sedimentation patterns. Therefore, $s(C)$ was estimated by the standard procedure to an accuracy of 5%. Both the pressure effect and the concentration effect were found to be negligible. The plot of $s(C)^{-1}$ against the polymer concentration C was fitted to the linear equation (8) as exemplified in Figure 7 for a series of poly(macromonomer) samples with a constant PS branch molecular weight of 2900, from which values of s at infinite dilution, s_0, and the concentration coefficient k_s were estimated and are given in Table 2.

$$s(C)^{-1} = s_0^{-1}(1 + k_s C) \tag{8}$$

Backbone Chain-Length Dependence of the Sedimentation Coefficient s_0. Figure 8 shows the M_w dependence of s_0 obtained from Figure 7. s_0 monotonically increases with M_w, while the slope tends to decrease with increasing M_w. s_0 is related to the

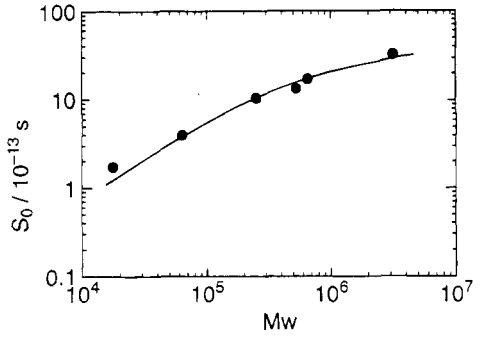

Figure 8. Dependence of s_0 on the PMMA backbone chain length. The solid curve is a calculated result using the prolate ellipsoid model 1-2.

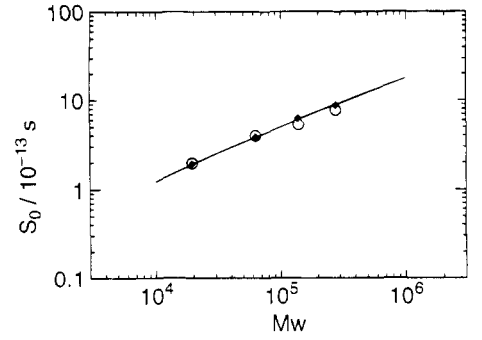

Figure 9. Dependence of s_0 on the PS branch length. The solid curve is a calculated result using the prolate ellipsoid model 1-2. The symbol ● has the same meaning as in Figure 6.

translational friction coefficient f_0 as given by the well-known formula eq 9.

$$s_0 = (1 - \bar{v}\varrho_0)M/N_A f_0 \tag{9}$$

where ϱ_0 and $\bar{v}$ are the solvent density and the specific volume of the poly(macromonomer) in benzene, respectively. The molecular weight dependence of s_0 is, aside from the term M in the numerator of the right-hand side of eq 9, essentially determined by the hydrodynamical variable f_0, just as D_0 is. Nevertheless, it should be pointed out that DLS measures the frictional property of the molecule at short time in the spatial scale of the wavelength of light, i.e., gives the short time diffusion coefficient, whereas SV proves the same property at long time in the macroscopic spatial scale to be related to the long time diffusion coefficient. Also, s_0 is a quantity independently obtained from the completely different experiment. Therefore, it seems worthwhile to examine the applicability of the prolate ellipsoid model 1-2 to the s_0 behavior using eqs 2, 3, and 9. Assuming the additivity of the specific volume as $\bar{v} = (0.9176M_{PS} + 0.8689M_{PMMA})/(M_{PS} + M_{PMMA})$ where M_{PMMA} is the molecular weight of the backbone, we obtain the solid curve in Figure 8. The agreement between experiment and model calculation looks gratifying, though data scattering around the curve is a little bit larger than that for D_0.

Branch-Length Dependence of s_0. The s_0 data of four poly(macromonomer) samples with $DP_{PMMA} \sim 20$ and varying M_{PS} from 800 to 14 000 are shown in Figure 9. The solid curve is a calculated result based on the prolate ellipsoid model 1-2. Once again we can reconfirm that the model gives s_0 values coincident with experimental values within an error of 10%. Good agreement for the lowest molecular weight sample is

in contrast with the disagreement observed for the D_0 behavior of the same sample and may cast a doubt about our supposition that the low molecular weight PS branch takes a fairly extended structure. Nevertheless, the D_0 and s_0 data clearly indicate that the whole shape of the poly(macromonomer) can be, to very good approximation, depicted as the prolate ellipsoid in which the PMMA backbone chain is extended so as to create space as wide as possible for accommodation of many PS branched chains. In a thermodynamic term, gain in entropy due to a Gaussian coil form of many PS chains is much larger than loss in entropy due to extension of one PMMA chain. This may give rise to an anisotropic structure of the poly(macromonomer) in dilute solution. The enthalpic interaction between styrene and methyl methacrylate monomers affects chain conformation in the vicinity of the backbone, but such a correlation in short spatial scale cannot be proved by either DLS or SV.

Discussion

Data Analysis in Terms of the Wormlike Cylinder Model. In previous sections, we showed that hydrodynamical properties of the poly(macromonomer) were well described by the prolate ellipsoid model 1-2 with extended PMMA chains. Objection may be raised to this conclusion, since PMMA is known as a flexible coil. In order to settle this issue, we attempted to estimate Kuhn's statistical length λ^{-1} by applying the wormlike cylinder model.

A theory developed by Norisuye et al.[26] is used here for data analysis. Their model is the wormlike cylinder capped with hemispheres at both ends, which is a refined one of the original model proposed by Yamakawa and Fujii.[27] The final expression for the translational friction coefficient f_0 reads as eq 10 with a form expanded in powers of d/L where L and d are the contour length and the diameter of the cylinder, respectively, and coefficients C_i ($i = 1-7$) are given as a function of d/L (eq 23 in ref 27).

$$3\pi\eta_0 L/f_0 = C_1 \ln(L/d) + C_2 + C_3(L\lambda) + C_4(L\lambda)^2 + C_5(L\lambda)^3 + C_6(L\lambda)^4 + C_7(L\lambda)^5 + \ldots \quad (10)$$

Equation 10 allows calculation of λ^{-1} when L, d, and f_0 are known. We put $L = 2a$ and $d = 2b$ to be consistent with the prolate ellipsoid model. We used the D_0 value of the highest molecular weight sample PM2900-1019 for an estimate of f_0 from the relation $f_0 = k_B T/D_0$, taking into account that the effect of chain flexibility becomes appreciable in the high molecular weight region. Substituting those values into eq 10, we found $\lambda^{-1} = 55$ nm to parameter values used for the ellipsoid model 1-1 and 84 nm for the model 1-2, respectively.

Once λ^{-1} is known, dependences of D_0 as well as of s_0 on the backbone chain length become calculable over the whole range of molecular weight studied. Figures 10 and 11 show comparisons of two theoretical curves with experimental data of D_0 and s_0, respectively. Obviously, the solid curve based on the parameter values of the model 1-2 reproduces the experimental findings much better than the dashed one, which once again supports the coiled form of the PS branches. $\lambda^{-1} = 84$ nm is about 25 times larger than that of syndiotactic homo-PMMA reported as 3.3 nm.[28] Therefore, we may be allowed to conclude that the PMMA backbone of the poly(macromonomer) is forced to take only an extended and pretty rigid conformation owing to the unique multibranched structure. This conclusion seems in harmony with the result of the Schmidt group, who reported $\lambda^{-1} = 100$ nm from the radius of gyration as well as DLS measurements on the same type of poly(macromonomer).[18]

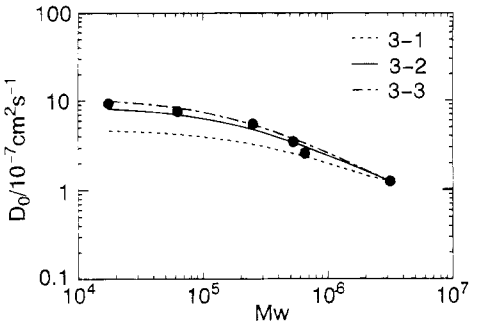

Figure 10. Wormlike cylinder model applied to the diffusion data shown in Figure 5 for an estimate of Kuhn's statistical length λ^{-1}. See text for values of parameters L, d, and λ^{-1} used for calculation of the three curves.

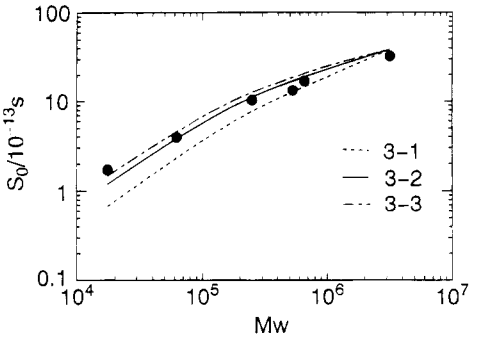

Figure 11. Applicability of the wormlike cylinder model to the sedimentation data shown in Figure 8 using the same parameter values used for the calculation of the three curves in Figure 10.

In Figure 1a, we observed that Γ_e/q^2 of the highest molecular weight sample PM2900-1019 increased with increasing scattering angle. The product of the contour length L and the scattering vector q becomes larger than unity above $\theta = 35°$ for this sample. Therefore, the intramolecular motion of the wormlike cylinder, probably the bending motion, contributes to a time profile of $A_q(t)$ at higher scattering angles in addition to the translational diffusion motion, resulting in the q dependence of Γ_e/q^2. The product qL is shown to be less than unity for other samples so that Γ_e/q^2 must be independent of q as observed.

We now examine the effect of the cylinder diameter on λ^{-1}. In the calculation of the diameter d in the model 1-2, the unperturbed dimension of PS given by eq 6 was used considering that the excluded-volume effect is small compared to that of the low molecular weight chain and also that PS branches are in the congested state. On the other hand, the ratio of R_G to the hydrodynamic radius R_H is 1.27 ± 0.03 for linear macromolecules in the Θ state.[20-23,29-31] If the hydrodynamic interaction would not be completely screened near the surface of the cylinder, the effective diameter of the cylinder might be smaller than $2\langle L_{PS}^2\rangle^{1/2}$. Using its minimum value of $2\langle L_{PS}^2\rangle^{1/2}/1.3$ as d, we recalculated D_0 and s_0, which are shown as the dash–dot curve with $\lambda^{-1} = 119$ nm in Figures 10 and 11, respectively. The dash–dot curve appears to describe the diffusion behavior successfully to the same extent as the solid curve with $\lambda^{-1} = 84$ nm does, but agreement is less satisfac-

tory for the sedimentation behavior. Though the above calculation corresponds to the extreme case, we had better to summarize that λ^{-1} is estimated as 90 nm within an uncertainty of 10 nm from our hydrodynamic measurements. Data of other hydrodynamical variables such as intrinsic viscosity are surely needed not only for a more accurate determination of L, d, and λ^{-1} but also for examination of the applicability of the model proposed here.

Concentration Coefficients k_D and k_s. Owing to the large experimental uncertainty of k_D and k_s, only a qualitative discussion will be given below. The second virial coefficient A_2 is related to k_D and k_s by eq 11.[32]

$$k_D + k_s + \bar{v} = 2A_2M \tag{11}$$

Since $\bar{v}$ is as small as about 1 cm^3 g^{-1}, the sign and magnitude of A_2 are determined by a sum of k_D and k_s. In substituting k_D and k_s values tabulated in Table 2 into eq 11, we find that A_2 of the PM2900 series increases from a negative value in the low molecular weight region to a positive one at higher molecular weights. On the other hand, A_2 of the samples with fixed DP_{PMMA} takes a minimum with increasing DP_{PS} at $DP_{PS} \sim DP_{PMMA}$ and then sharply increases compared with the former series. These properties should be considered as one of the characteristics of the poly(macromonomer) and await more detailed theoretical analysis.

The coefficient k_s of linear polymers is often discussed in terms of the hydrodynamic volume v_H as eq 12.[33-45]

$$k_s = BN_Av_H/M_w \tag{12}$$

The numerical coefficient B ranges from 6.55 to 7.19 in a good solvent and from 1.0 to 2.23 in a Θ state. We estimated B of the poly(macromonomer), applying the prolate ellipsoid model for which $v_H = (4\pi/3)ab^2$. For the PM-2900 series, B was found to remain less than 3 in the low-M_w region and then increased up to 25 (this value is subject to large experimental error). For another series, B looked to take a minimum at $DP_{PS} \sim DP_{PMMA}$ and then increased to 11. Thus the behavior is quite different from that found for linear polymers.

Acknowledgment. We are very grateful to Prof. Y. Tsukahara of KIT for a gift of very valuable poly(macromonomer) samples. Thanks are also tendered to Profs. K. Osaki, S. Kohjiya, and T. Yosizaki of Kyoto University and to Prof. T. Norisuye of Osaka University for valuable discussion. We also thank K. Itoh for his help in data analysis.

References and Notes

(1) Schmidt, M.; Nerger, D.; Burchard, W. *Polymer* **1979**, *20*, 582.
(2) Kajiwara, K.; Burchard, W. *Polymer* **1981**, *22*, 1621.
(3) Roovers, J.; Toporowski, P. M. *J. Polym. Sci., Polym. Phys. Ed.* **1980**, *18*, 1907.
(4) Burchard, W.; Schmidt, M.; Stockmayer, W. H. *Macromolecules* **1980**, *13*, 1265.
(5) Huber, K.; Burchard, W.; Fetters, L. J. *Macromolecules* **1984**, *17*, 1265.
(6) Noda, I.; Horikawa, T.; Kato, T.; Fujimoto, T.; Nagasawa, M. *Macromolecules* **1970**, *3*, 795.
(7) Rempp, R.; Franta, E.; Masson, P.; Lutz, P. *Prog. Colloid Polym. Sci.* **1986**, *72*, 112.
(8) Tsukahara, Y.; Mizuno, K.; Segawa, A.; Yamashita, Y. *Macromolecules* **1989**, *22*, 1546.
(9) Tsukahara, Y.; Tsutsumi, K.; Yamashita, Y.; Simada, S. *Macromolecules* **1990**, *23*, 5201.
(10) Tsukahara, Y. *Macromolecular Design: Concept and Practice*; Mishra M., Ed.; Polymer Frontiers International, Inc.: New York, 1993; p 161.
(11) Ito, K.; Tomi, Y.; Kawaguchi, S. *Macromolecules* **1992**, *25*, 1534.
(12) Tomalia, D. A.; Baker, H.; Dewald, J.; Hall, M.; Kallos, G.; Martin, S.; Roeck, J.; Ryder, J.; Smith, P. *Polym. J.* **1985**, *17*, 117.
(13) Tomalia, D. A.; Naylor, A. M.; Goddard, W. A., III *Angew. Chem., Int. Ed. Engl.* **1990**, *29*, 138.
(14) Hawker, C. J.; Frechet, J. M. *Macromolecules* **1990**, *23*, 4726.
(15) Mansfield, M. C.; Klushin, L. I. *J. Phys. Chem.* **1992**, *96*, 3994.
(16) Mourey, T. H.; Turner, S. R.; Rubinstein, M.; Frechet, J. M.; Hawker, C. J.; Wooley, K. L. *Macromolecules* **1992**, *25*, 2401.
(17) Tsukahara, Y.; Kohjiya, S.; Tsutsumi, K.; Okamoto, Y. *Macromolecules* **1994**, *27*, 1662.
(18) Wintermantel, M.; Schmidt, M.; Tsukahara, Y.; Kajiwara, K.; Kohjiya, S. *Macromol. Rapid Commun.* **1994**, *15*, 279.
(19) Nemoto, N.; Kuwahara, M. *Langmuir* **1993**, *9*, 419.
(20) Tsunashima, Y.; Nemoto, N.; Kurata, M. *Macromolecules* **1983**, *16*, 1184.
(21) Nemoto, N.; Makita, M.; Tsunashima, Y.; Kurata, M. *Macromolecules* **1984**, *17*, 425.
(22) Tsunashima, Y.; Hirata, M.; Nemoto, N.; Kurata, M. *Macromolecules* **1987**, *20*, 1992.
(23) Tsunashima, Y.; Hirata, M.; Nemoto, N.; Kajiwara, K.; Kurata, M. *Macromolecules* **1987**, *20*, 2862.
(24) Berne, B. J.; Pecora, R. *Dynamic Light Scattering*; Wiley: New York, 1976.
(25) Kurata, M.; Tsunashima, Y. *Polymer Handbook*, 3rd ed.; Brandrup, J., Immergut, E. H., Eds.; Wiley: New York, VII-1.
(26) Norisuye, T.; Motowoka, M.; Fujita, H. *Macromolecules* **1979**, *12*, 320.
(27) Yamakawa, H.; Fujii, M. *Macromolecules* **1973**, *3*, 407.
(28) Yamakawa, H. *Annu. Rev. Phys. Chem.* **1984**, *35*, 23.
(29) Schmidt, M.; Burchard, W. *Macromolecules* **1981**, *14*, 210.
(30) Han, C. C.; Akcasu, A. Z. *Macromolecules* **1981**, *14*, 1080.
(31) Konishi, T.; Yoshizaki, T.; Yamakawa, H. **1991**, *24*, 5614.
(32) See, for example: Yamakawa, H. *Modern Theory of Polymer Solutions*; Harper & Row: New York, 1971.
(33) Pyun, C. W.; Fixman, M. *J. Chem. Phys.* **1964**, *41*, 937.
(34) Yamakawa, H. *J. Chem. Phys.* **1962**, *36*, 2995.
(35) Imai, S. *J. Chem. Phys.* **1970**, *52*, 4212.
(36) Mulderije, J. J. H. *Macromolecules* **1980**, *13*, 1207, 1526.
(37) Akcasu, A. Z.; Benmouna, M. *Macromolecules* **1978**, *11*, 1193.
(38) Akcasu, A. Z. *Polymer* **1981**, *22*, 1169.
(39) King, T. A.; Knox, A.; Lew, W. I.; McAdam, J. D. *Polymer* **1973**, *14*, 151.
(40) Han, C. C. *Polymer* **1979**, *20*, 259.
(41) Jones, G.; Caroline, D. *J. Chem. Phys.* **1979**, *37*, 187.
(42) Tsunashima, Y.; Nemoto, N. *Macromolecules* **1983**, *16*, 1941.
(43) Tsunashima, Y.; Nemoto, N. *Macromolecules* **1984**, *17*, 2931.
(44) Varma, B. K.; Fujita, Y.; Takahashi, M.; Nose, T. *J. Polym. Sci., Polym. Phys. Ed.* **1984**, *22*, 1781.
(45) Huber, K.; Bantle, S.; Lutz, P.; Burchard, W. *Macromolecules* **1985**, *18*, 1461.

MA946532F